JPL Publication 14-18

Geostationary Coastal and Air Pollution Events (GEO-CAPE) Sensitivity Analysis Experiment

Meemong Lee and Kevin Bowman

National Aeronautics and Space Administration

Jet Propulsion Laboratory
California Institute of Technology
Pasadena, California

October 2014

The research described in this publication was carried out at the Jet Propulsion Laboratory, California Institute of Technology, under a contract with the National Aeronautics and Space Administration.

Reference herein to any specific commercial product, process, or service by trade name, trademark, manufacturer, or otherwise does not constitute or imply its endorsement by the United States Government or the Jet Propulsion Laboratory, California Institute of Technology.

© 2014 California Institute of Technology. Government sponsorship acknowledged

Table of Contents

1 Introduction 1

2 Adjoint Sensitivity Analysis Framework 2

2.1 Emission Inventory 2
2.2 Cost Function and Gradient Cost Function 3
2.3 Software Process 5
2.4 Adjoint-Sensitivity Configuration 6

3 Model Parameters 8

4 Sensitivity Analysis Experiments 11

4.1 Sensitivity Analysis of Observation Scenarios 12
4.2 Sensitivity Analysis of Instrument Options 20

5 Appendices 22

Appendix A. Checkpoint files 22
Appendix B. NOx Emission Inventory 23
Appendix C. Tracer name list 24
Appendix D. Acronyms and Abbreviations 26

Figures

Figure 1. Adjoint Sensitivity Analysis Framework 2
Figure 2. Adjoint Sensitivity Analysis Processes 6
Figure 3. External Configuration of the Sensitivity Function 7
Figure 4. NOX emission sources over N. America in 2006/08 9
Figure 5. Total Anthropogenic NOx Emission and Diurnal Scale Factor of Five Fuel Combustion Sources 10
Figure 6. Weekly Mean Ozone Sensitivity to the Global NOx Emissions during One Month (2006/May) 11
Figure 7. CASTNet Sites (red squares) and EPA Region 9 (California, Arizona, & Nevada shown in pinkish highlight) 12
Figure 8. Analysis Regions Marked in Dotted Circle on the Global NOx Emission Background 12
Figure 9. Five Regions of the NOx Emission and Daily Contribution Ratios during 2006/05 to USA O_3 13
Figure 10. Sensitivity Comparison between Observations at the EPA-9 Region and at CASTNet Sites 14
Figure 11. Column O_3 over the EPA-09 Region (Top) and Contributions from NOx Emissions (Bottom) 15
Figure 12. Column O_3 over the EPA-09 Region (Top) and Contributions from NOx Emissions (Bottom) 16
Figure 13. The Column O_3 change in EPA-09 region due to NOx emissions from EPA09 and China for 2006/05 (Top) and 2006/05/20 (Bottom) 17
Figure 14. Sensitivity Comparison between the Surface O_3 (Top) and Column O_3 Observations (Bottom) 18
Figure 15. Sensitivity to the State-Wide NOx Emission: Surface O_3 (top) and Column O_3 (Bottom) 19
Figure 16. Diagonal Vector of the Averaging Kernel of Three Instruments 20
Figure 17. Sensitivity Comparison of the Three Instruments Relative to an Ideal Instrument 21

Tables

Table 1. Sensitivity Analysis Study Cases 1
Table 2. Emission Inventories 3
Table 3. 57 Emissions Mapped to the Tracers and the Emission Types 8

1 Introduction

GEO-CAPE is a NASA decadal survey mission to be designed to provide surface reflectance at high spectral, spatial, and temporal resolutions from a geostationary orbit necessary for studying regional-scale air quality issues and their impact on global atmospheric composition processes. GEO-CAPE's Atmospheric Science Questions explore the influence of both gases and particles on air quality, atmospheric composition, and climate [http://geo-cape.larc.nasa.gov/atmosphere].

1. What are the temporal and spatial variations of emissions of gases and aerosols that are important for air quality and climate?
2. How do physical, chemical, and dynamical processes determine tropospheric composition and air quality over scales ranging from urban to continental, diurnally to seasonally?
3. How does air pollution drive climate forcing, and how does climate change affect air quality on a continental scale?
4. How can observations from space improve air quality forecasts and assessments for societal benefit?
5. How does intercontinental transport affect surface air quality?
6. How do episodic events (such as wild fires, dust outbreaks, and volcanic eruptions) affect atmospheric composition and air quality?

The GEO-CAPE Observing System Simulation Experiment (OSSE) team at JPL has developed a comprehensive sensitivity analysis framework to quantitatively evaluate the impact of the GEO-CAPE observations. Employing the sensitivity framework, a wide range of OSSEs have been performed varying the target location, analysis region and duration, and evaluation criteria as illustrated in Table 1 with four study cases. This report describes the mathematical and computational processes of the sensitivity analysis framework and discusses the findings with respect to the OSSE configuration and the sensitivity of the observed ozone to NOx surface emissions.

Table 1. Sensitivity Analysis Study Cases

Case	Target location	Analysis region	Analysis duration	Evaluation	Resolution
1	N. America	N. America	2006/08/01-06	57 Emission types	0.5 ° × 0.667°
2	Washington D.C.	N. America	2006/07/21-26	TIR, UV, VIS	0.5 ° × 0.667°
3	USA	Global	2006/05/01-31	GEO-CAPE, CASTNet	2° × 2.5°
4	EPA-09 region	Global	2006/05/01-31	Surface O_3, Column O_3	2° × 2.5°

2 Adjoint Sensitivity Analysis Framework

The Adjoint Sensitivity Analysis framework was developed based on the GEOS-Chem-Adjoint version 34 system (GCA), which provides the adjoint models for dynamics, emission, and chemistry. Figure 1 describes the relationship between the forecast loop and the adjoint loop during the sensitivity analysis process. The forecast loop simulates the state of the atmospheric composition forward in time and saves the checkpoint files (Appendix A) required for the adjoint loop at each simulation time. The adjoint loop computes a sensitivity function of the target observation (described in an observation scenario) and propagates the sensitivity backward in time employing the adjoint models.

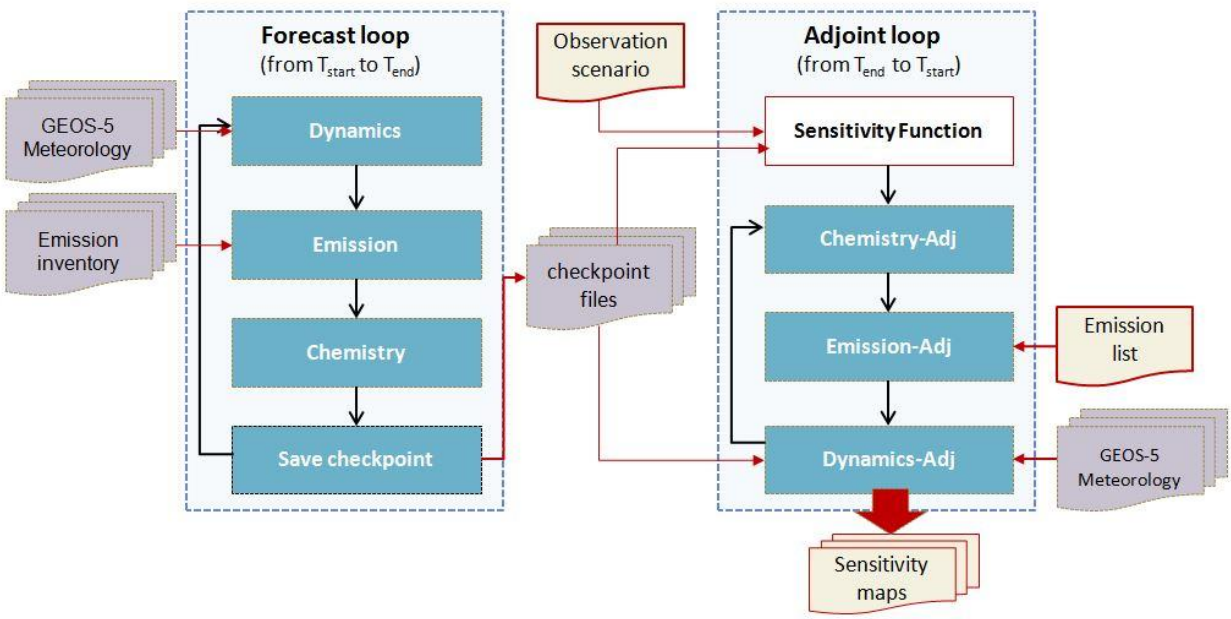

Figure 1. Adjoint Sensitivity Analysis Framework

2.1 Emission Inventory

The Emission Inventory is organized for anthropogenic and biogenic groups as summarized in Table 2. The anthropogenic group includes emissions from the human activities on land, air, and ocean. The biogenic group includes emission sources and sinks from plant, soil, lightning, and fire. There are five global inventories and five regional inventories for the anthropogenic emissions. Also additional inventories are available for emissions from aircraft, shipping, and bio-fuel. Each emission is scaled by a set of temporal scale factors (e.g., annual, seasonal, weekday, weekend, and hourly) and/or a set of spatial scale factors (e.g., soil type and leaf area index). The emissions within each model are organized in multiple sectors with sector-specific temporal scale factors and applicability regions (Appendix B).

At each simulation time step, the GCA forecasts the state of 43 tracers (33 chemical components and 10 aerosol compounds as shown in Appendix C) with the dynamics model, emission model, and chemical processing model. The dynamics model performs the advection process and the convection process based on the GEOS-5 meteorology fields generated by the Goddard Earth Observing System (GEOS) version 5.

Table 2. Emission Inventories

Type	Model	Scale	Misc. description
Anthro-global	EMEP	annual	Europe
	EDGAR v4.2	hourly	
	NEI2005	seasonal	USA
	RETRO	IPCC future	
Anthro-regional	STREETS	monthly	SE Asia
	CAC		Canada
	Bravo		Mexico
	Cooke GC/OC		N. America
Aircraft			
Ship	ICOADS		
Biofuel			
Plant	MEGAN		AEF_ISOP, AEF_MONOT
			Leaf_area_index
Biomass burn	GFED2	Monthly	
	GFED3 (optional)	3 hourly	
Lightning		Scale, loc_redist, CTH param	NOx
Soil	Olson	Fertilizer	NOx

Acronyms used in this table are explained in Appendix D.

2.2 Cost Function and Gradient Cost Function

The mathematical definition of the cost function and gradient cost function within the adjoint sensitivity framework is described below following the work of Henze et al.[1]

The adjoint model is used to calculate gradients of the error weighted squared difference between model predictions and observations with respect to emissions. An adjoint model is an efficient means of calculating the sensitivities of this type of model response with respect to numerous model parameters simultaneously, affording optimization of parameters on a resolution commensurate with that of the forward model itself. This allows refinement of both the overall magnitude and the spatial distributions of emissions, distinguishing between different emission source sectors, and quantification of the influence of other uncertain model parameters such as initial conditions and heterogeneous uptake coefficients.

A chemical transport model can be viewed as a numerical operator, F, acting on a vector of initial concentrations, c^0, and a vector of parameters, p, to yield an estimate of the evolved concentrations at a later time, N,

[1] D. K. Henze, J. H. Seinfeld, and D. T. Shindell, "Inverse modeling and mapping US air quality influences of inorganic $PM_{2.5}$ precursor emissions using the adjoint of GEOS-Chem," *Atmos. Chem. Phys.*, vol. 9, pp. 5877–5903, 2009.

$$c^N = F(c^0, \mathrm{p}) \tag{1}$$

where c is the vector of all K tracer concentrations, $c = [c_1, \ldots, c_k, \ldots, c_K]$ and c^n is the concentration at time step n. In practice, F comprises many individual operators representing various physical processes. For the moment, let F^n represent a portion of the discrete forward model that advances the concentration vector from time step n to step $n + 1$.

$$c^{n+1} = F^n(c^n, p), \tag{2}$$

The adjoint model is used to calculate the sensitivity of a scalar model response function, J, with respect to the model parameters, p. The response function may depend only upon a subset of concentrations, , J^n J_p, and may include a term explicitly depending upon the parameters.

$$\mathrm{J} = \sum_{n\in\ \ _n} J^n\,(\hat{c}^n) + J_p(p) \tag{3}$$

Assuming the parameters are constants, J_p (p) does not have a time step index. In practice the definitions of , J^n J_p are very application-specific. For the following derivation it is simply assumed that the response domain includes all species at all times and the parameters are constant, such that

$$\mathrm{J} = \sum_0^N j^n\,(c^n) + J_p(p) \tag{4}$$

The purpose of the adjoint model is to calculate the sensitivity of the response with respect to the model parameters. As will become evident, it is first necessary to calculate the sensitivity of the model response with respect to species concentrations at every time step n in the model,

$$\nabla_{\mathrm{c}^{\mathrm{n}}} J = \left(\frac{\partial J}{\partial c}\right)^T = \sum_{n=n}^{N} \left(\frac{\partial j^n}{\partial c^n}\right)^T \tag{5}$$

note: $\frac{\partial j^n}{\partial c^n} = 0$ when n' < n

The Jacobian matrix of the model operator around any given time step can be written as and similarly,

$$\partial c^{n+1} / \partial c^n = \partial F^n(c^n)/\partial c^n = \boldsymbol{F}_c^n \tag{6}$$

$$\partial c^{n+1} / \partial p = \partial F^n(c^n)/\partial p = \boldsymbol{F}_p^n \tag{7}$$

Using the chain rule, the sum on the right hand side of Eq. (5) is expanded,

$$\begin{aligned}\nabla_{c^n} J = {} & (\boldsymbol{F}_c^n)^T (\boldsymbol{F}_c^{n+1})^T (\boldsymbol{F}_c^{N-1})^T \left(\frac{\partial J^N}{\partial c^N}\right)^T \\ & + (\boldsymbol{F}_c^n)^T (\boldsymbol{F}_c^{n+1})^T (\boldsymbol{F}_c^{N-2})^T \left(\frac{\partial J^{N-1}}{\partial c^{N-1}}\right)^T + \cdots \\ & + \left(\frac{\partial J^n}{\partial c^n}\right)^T\end{aligned} \tag{8}$$

The sensitivity of the response with respect to the model parameters (assumed here not to depend on the time step n) can then be written as

$$\begin{aligned}\nabla_p \mathrm{J} = {} & (\mathbf{F}_{\mathrm{p}}^{\mathrm{N}-1})^{\mathrm{T}}\ \nabla_{\mathrm{c}^{\mathrm{N}}} \mathrm{J} \\ & + (\mathbf{F}_{\mathrm{p}}^{\mathrm{N}-2})^{\mathrm{T}}\ \nabla_{\mathrm{c}^{\mathrm{N}-1}} \mathrm{J} + \cdots\end{aligned}$$

$$+ (\mathbf{F}_p^0)^T \ \nabla_{c^1} J \ + (\frac{\partial J_p}{\partial p})^T \qquad (9)$$

In this context, the adjoint method is essentially just an approach to evaluating Eqs. (8) and (9), that is computationally efficient when dim{c} and dim{p} > dim {J }. The adjoint sensitivity variables are defined as $\lambda_c^n = \Delta_{cn}J$ and $\lambda_p = \Delta_p J$, where the subscripts c and p indicate sensitivity with respect to c and p, respectively. Initializing

$$\begin{aligned} \nabla_p J = & (\mathbf{F}_p^{N-1})^T \ \nabla_{c^N} J \\ & + (\mathbf{F}_p^{N-2})^T \ \nabla_{c^{N-1}} J \ + \cdots \\ & + (\mathbf{F}_p^0)^T \ \nabla_{c^1} J \ + (\frac{\partial J_p}{\partial p})^T \end{aligned} \qquad (9)$$

adjoint sensitivities are found by evaluating the following update formulas iteratively from n = N, . . ., 1

$$\lambda_c^{n-1} \ = (\boldsymbol{F}_c^{n-1})^T \ \lambda_c^n \ + (\frac{\partial J^{n-1}}{\partial c^{n-1}})^T \qquad (10)$$

$$\lambda_p \ = (\boldsymbol{F}_p^{n+1})^T \lambda_c \ + \ \lambda_p \qquad (11)$$

The $\frac{\partial J^n}{\partial c^n}$ terms are referred to as the adjoint forcings as their role in the adjoint model is analogous to that of emissions in the forward model. While calculation of adjoint values using this algorithm is straightforward, there are a few subtleties worth mentioning. First, evaluating sensitivities with respect to model parameters requires having first calculated sensitivities with respect to concentrations. Since evaluation of Eq. (8) is much more computationally expensive than evaluation of Eq. (9), the overall computational cost is largely invariant to the number of parameters considered. Second, while solving Eq. (11) iteratively along with Eq. (10) is not necessary, it is computationally preferable as values of λ_c^n and $\boldsymbol{F}_p^n$ need not be stored for more than a single step.

2.3 Software Process

The sensitivity analysis framework has extended the GCA software system to support external configuration of the cost function and to track intermediate stage of the gradient cost array and emission status. The extension required a careful mapping between the adjoint sensitivity function described above and the data variables inside of the GCA software implementation. Figure 2 describes the process flow of the adjoint loop within the GCA framework, which includes the six steps described below:

- Step 1: The sensitivity function (CALC_ADJ_FORCE) computes the cost and adjoint force, and updates the total cost and the gradient cost array (CSPEC_ADJ).
- Step 2: The chemistry adjoint process derives two types of sensitivities from the adjoint force, a sensitivity with respect to concentration and a sensitivity with respect to the reaction rate coefficient.

- Step 3: The emission rate (REMIS_ADJ) is derived from the sensitivity with respect to the reaction rate coefficient.
- Step 4: The emission adjoint process extracts the emissions (E) from the emission inventory for the time step of the adjoint loop.
- Step 5: Prior to the dynamics adjoint process, the gradient cost array is partitioned to a model grid array (STT_ADJ). Then, the dynamics adjoint process (PBLMIX, CONVECTION, and TRANSPORT) is applied to tracer the winds backward. After the dynamics adjoint process, the model grid array is lumped back to the gradient cost array.
- Step 6: The emission sensitivity array (EMS_SF_ADJ) is populated by multiplying the emissions to the emission rates, and saved hourly for post processing.

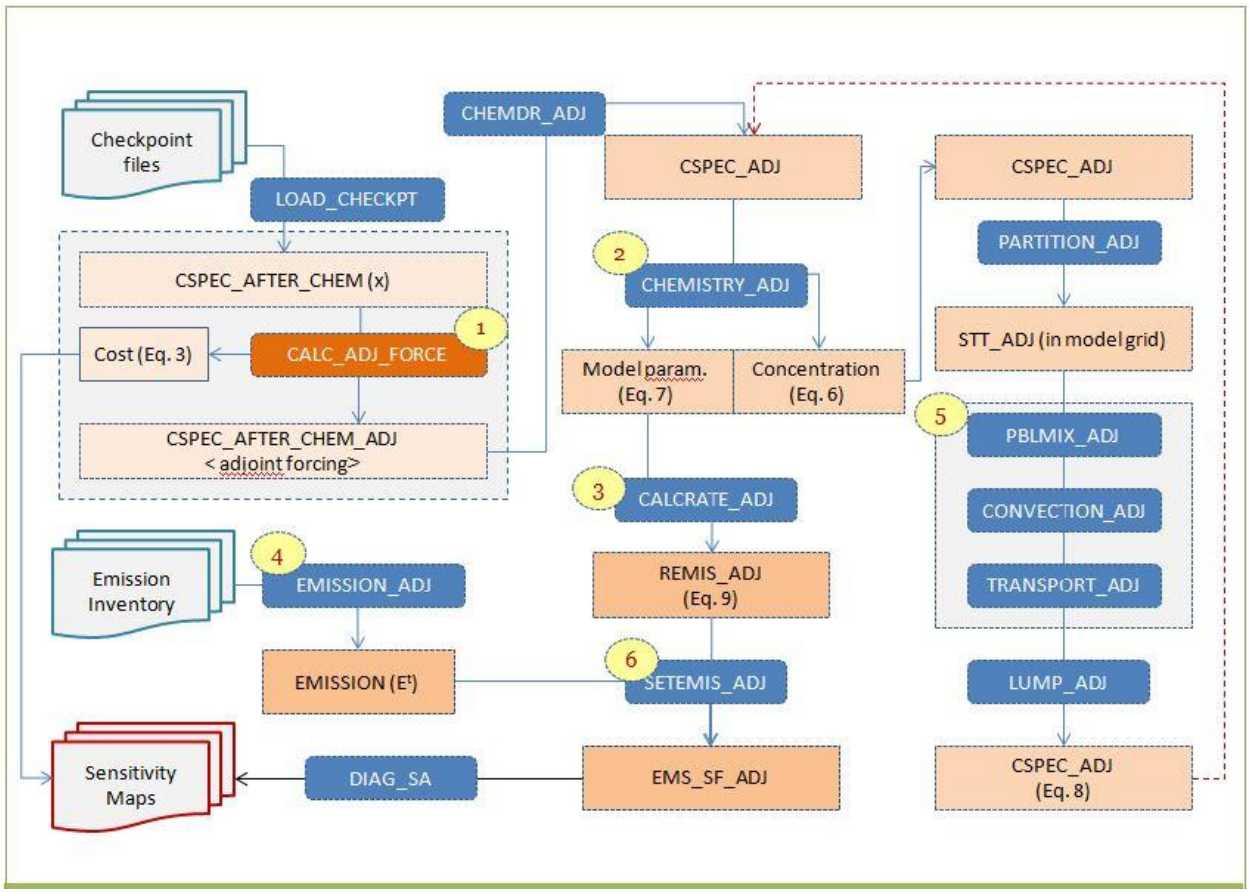

Figure 2. Adjoint Sensitivity Analysis Processes

2.4 Adjoint-Sensitivity Configuration

The adjoint model is used to calculate the sensitivity of a scalar model response function, J, with respect to the model parameters, p. The response function may depend only upon a subset of concentrations (the subset applies to temporal range, areal region, or chemical species) and may include a term explicitly depending upon the parameters. In this study, the model parameters are set to be the emission types.

The sensitivity function has been implemented to accept four types of control parameters, a time range, a sample list, a pressure range, and an averaging kernel to explore the impact of sampling scenarios and instrument options. As shown in Figure3, a target location is represented with a sample list which specifies the sample locations in latitude and longitude and a time range during which the observations should be made. The time range can also be applied during the evaluation of the instrument options.

- Cost type 1: The cost of the tracer O_3 is defined to be the mean concentration in the unit of parts per billion (ppb) where the O_3 concentration is retrieved from the CSPEC array (values are stored in molecules/cm^3).
- Cost type 2: The cost of the tracer O_3 is defined to be the sum of the concentration within the target area in the unit of ppb where the O_3 concentration is retrieved from the STT array (values are stored in v/v).

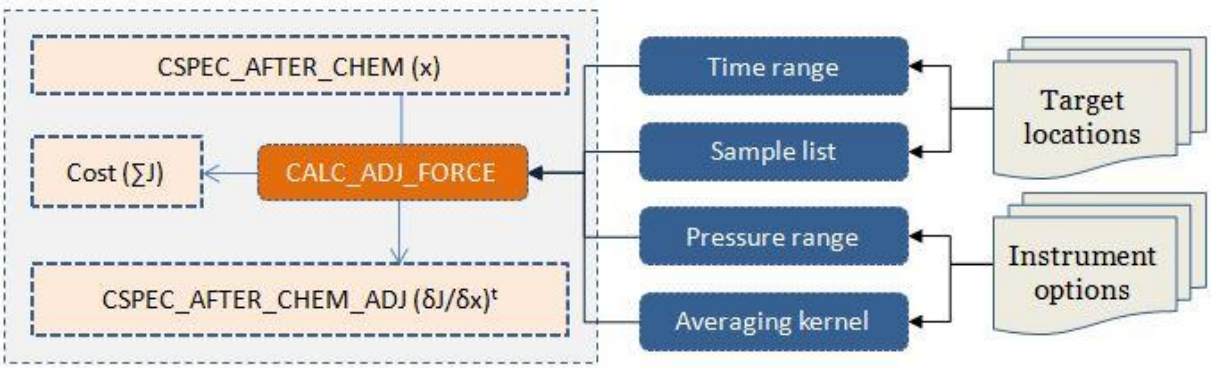

Figure 3. External Configuration of the Sensitivity Function

3 Model Parameters

In general, the parameters of a chemical transport model include emissions, boundary conditions, initial conditions, and rate parameters for deposition and chemical reactions. For this study, the parameters initially considered are scaling factors for the emissions of SO_x, NO_x, and NH_3 from the source sectors listed in Table 2. The emissions extracted from the emission inventories are internally organized into a two-dimensional emission array (E), the relevant tracers for the first dimension and the emission type for the second dimension.

Currently there are 57 emissions and Table 3 shows their mapping to the two dimensional array composed of the tracers and the emission types. Figure 4 shows the spatial distribution and magnitude range (in moles/cm^2/s) of the six emission types in North America. Figure 5 shows the spatial distribution of the global anthropogenic NOx and associated diurnal signatures of five major anthropogenic sources, road and non-road transportations, industry, power generation, and residential.

Table 3. 57 Emissions Mapped to the Tracers and the Emission Types

Tracer*	anthro	biofuel	Aircraft/ship	Plant	Biomass burn	lightning	soil
NOx	25	26	24		27	23	22
CO	38	29			30		
ALK4	34	35			36		
ISOP	31	32			33		
ACET	37	38			39		
MEK	40	41			42		
ALD2	43	44			45		
PRPE	46	47			48		
C_3H_8	49	50			51		
C_2H_6	55	56			57		
SO_2	5,6	7	9		8		
NH_3	1	4		2	3		
BCPI	10	14			18		
OCPI	12	16			20		
BCPO	11	15			19		
OCPO	13	17			21		

Note: Appendix C lists the full names of the tracers listed in the first column.

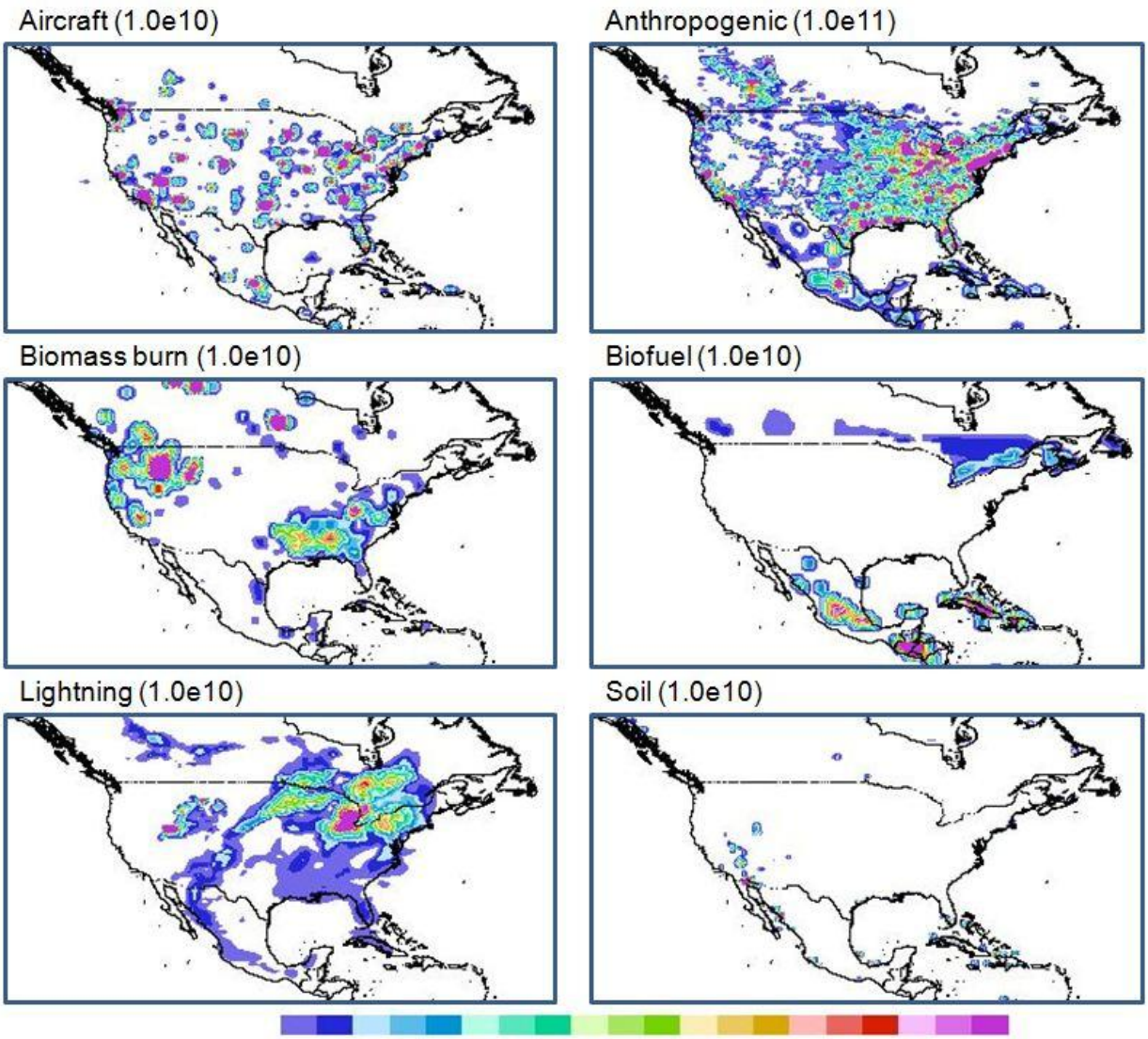

Figure 4. NOX emission sources over N. America in 2006/08

(The value range of the color bar is between 0 and the value shown in parenthesis next to each emission type.)

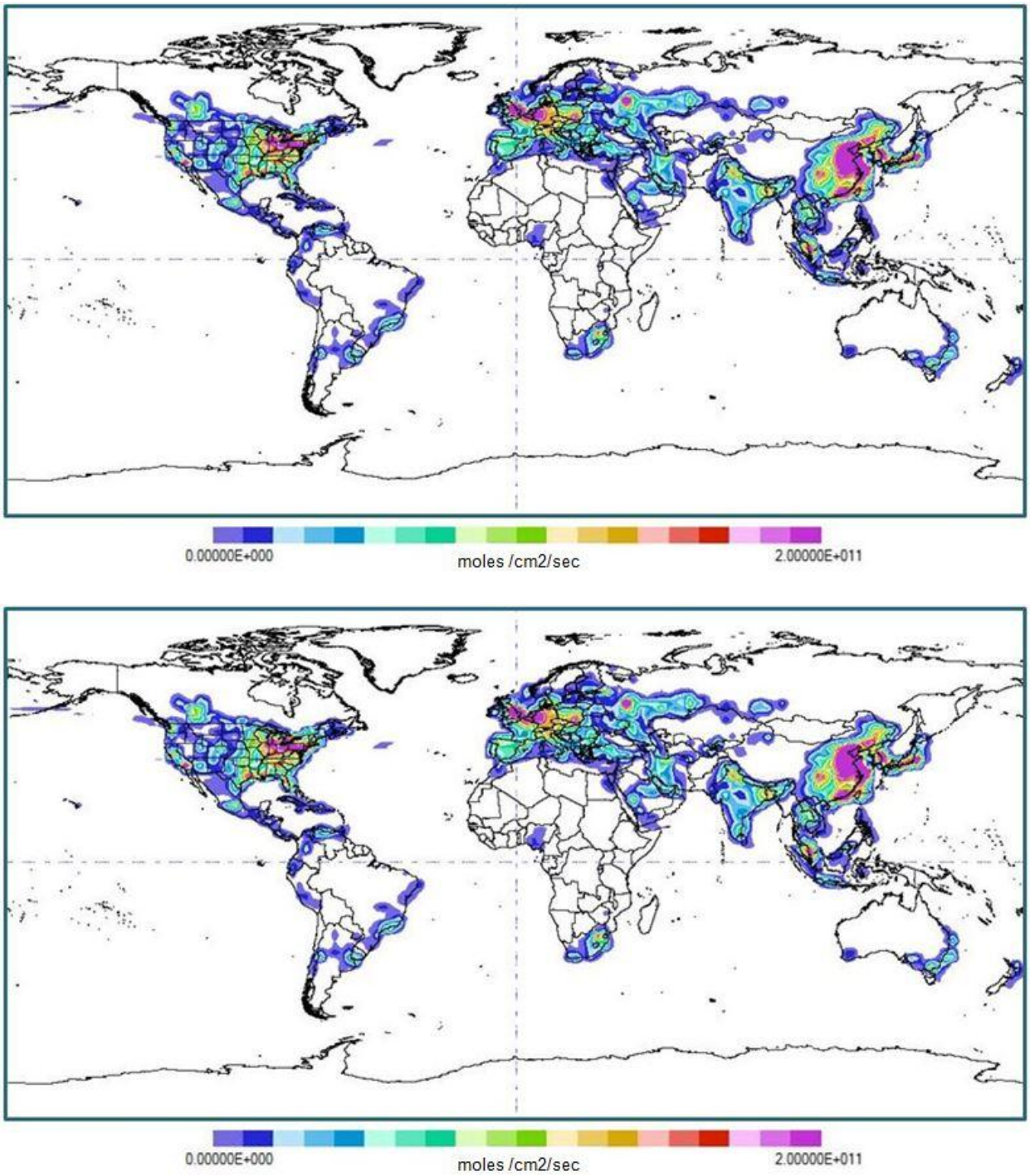

Figure 5. Total Anthropogenic NOx Emission and Diurnal Scale Factor of Five Fuel Combustion Sources

(The road and non-road transportation sources have identical diurnal signature with two sharp peaks corresponding to the commute times.)

4 Sensitivity Analysis Experiments

The NOx emission sensitivity analysis tracks the adjoint sensitivity stored in the EMS_SF_ADJ variable hourly, integrating the sensitivities for the three types of NOx emission sources, anthropogenic, bio-fuel, and biomass-burn. The NOx emissions from aircraft, lightning, and soil are not included for the analysis. Figure 6 illustrates the weekly mean sensitivities of the continental United States ozone (CONUS--O_3) during one month (2006/05) to the global NOx emissions. As the assimilation process progresses backward in time starting on May/31, 2006, the impact of the global NOx emissions starts to appear. The impact of the NOx emissions in China starts in the second week, and it exceeds the impact of the NOx emissions in the EPA-9 region.

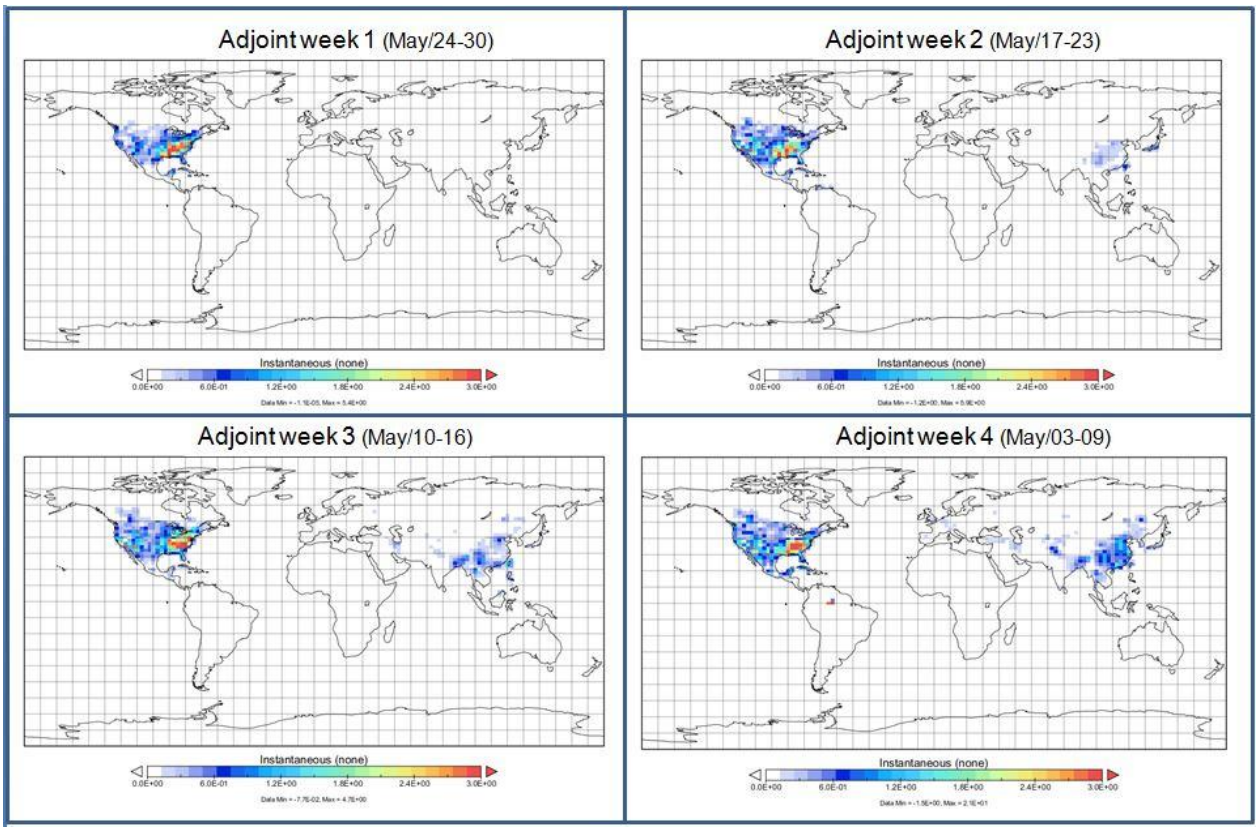

Figure 6. Weekly Mean Ozone Sensitivity to the Global NOx Emissions during One Month (2006/May)

The impact of an observation scenario can be evaluated by performing the above sensitivity analysis and analyzing the temporal and spatial relationships of the resulting sensitivity results. Section 4.1 discusses the OSSEs performed for seven observation scenarios to quantify the impact of their sampling strategies. Section 4.2 discusses the OSSES performed for three instrument systems to quantify the impact of their averaging kernels.

4.1 Sensitivity Analysis of Observation Scenarios

The sensitivity of the ozone to the NOx emissions was evaluated for two regions, the EPA-9 region and the CONUS region. For each region, the samples were simulated for two levels of sampling densities, an entire region and only at the CASTNet sites within the region. The locations of the CASTNet sites mapped to the 2° × 2.5° GCA model grid are shown as red squares and the EPA-09 region (California, Arizona, and Nevada) is painted in pink in Figure 7. The regional contribution of the sensitivity was analyzed by integrating the sensitivity over the five regions, EPA-09, China, India, North East Asia, and South East Asia as shown in Figure 8. Figures 9 through 15 show _____. [a short phrase will do to callout the figures.]

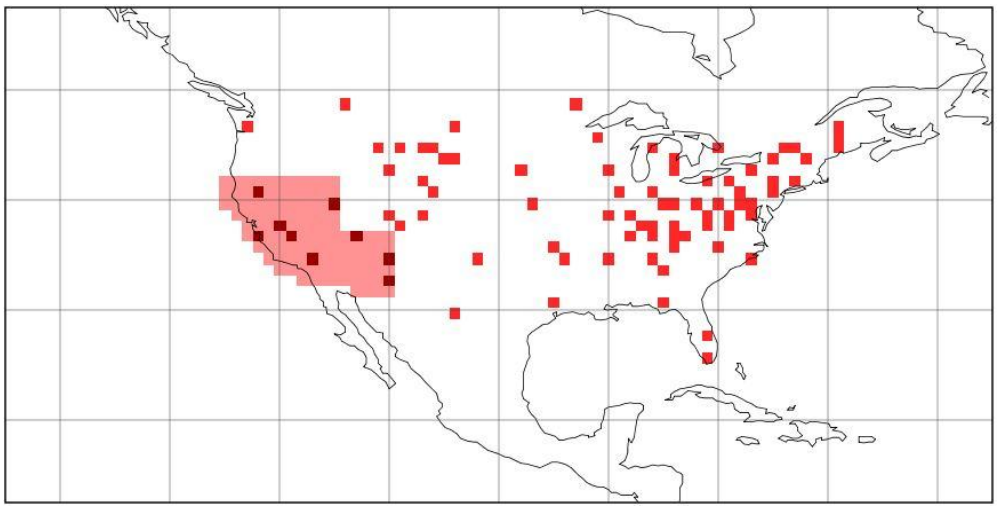

Figure 7. CASTNet Sites (red squares) and EPA Region 9 (California, Arizona, & Nevada shown in pinkish highlight)

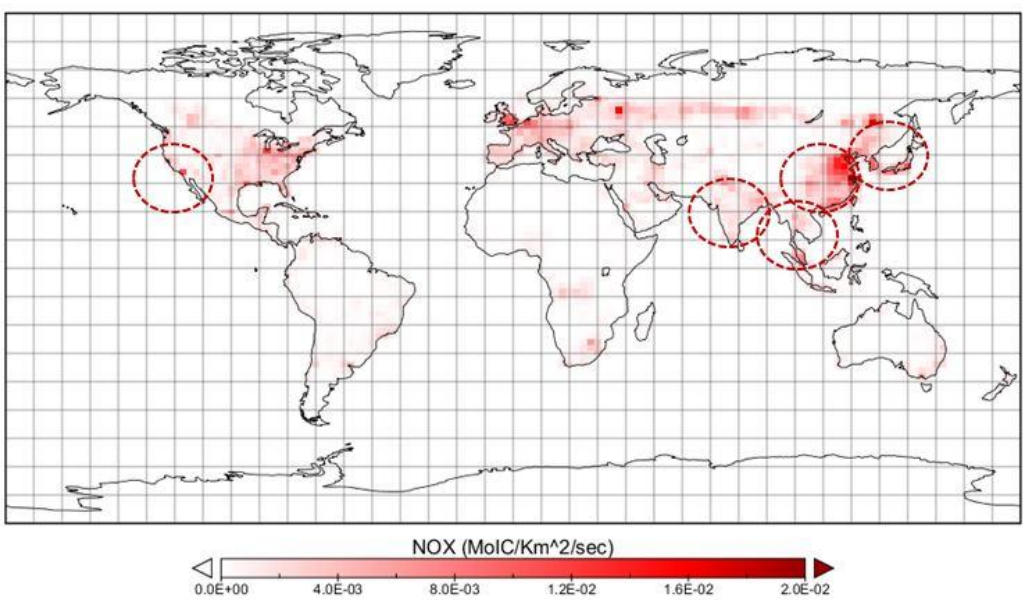

Figure 8. Analysis Regions Marked in Dotted Circle on the Global NOx Emission Background

Observations	**Column O_3 (hourly during May of 2006)**
Target area	**USA (93 CASTNet sites)**
Analysis duration	**2006/05/01-30**
Analysis regions	**EPA-9, China, India, North East Asia, South East Asia**

Findings:

1. The sensitivity to the EPA-9-NOx stays about constant over the entire month.
2. It takes ~8 days for the Chinese NOx emission starts to impact the USA O3 and it has higher impact than the EPA-9 NOx emission.
3. The sensitivity to the Chinese NOx emission dominates the sensitivities to other regions in Asia.

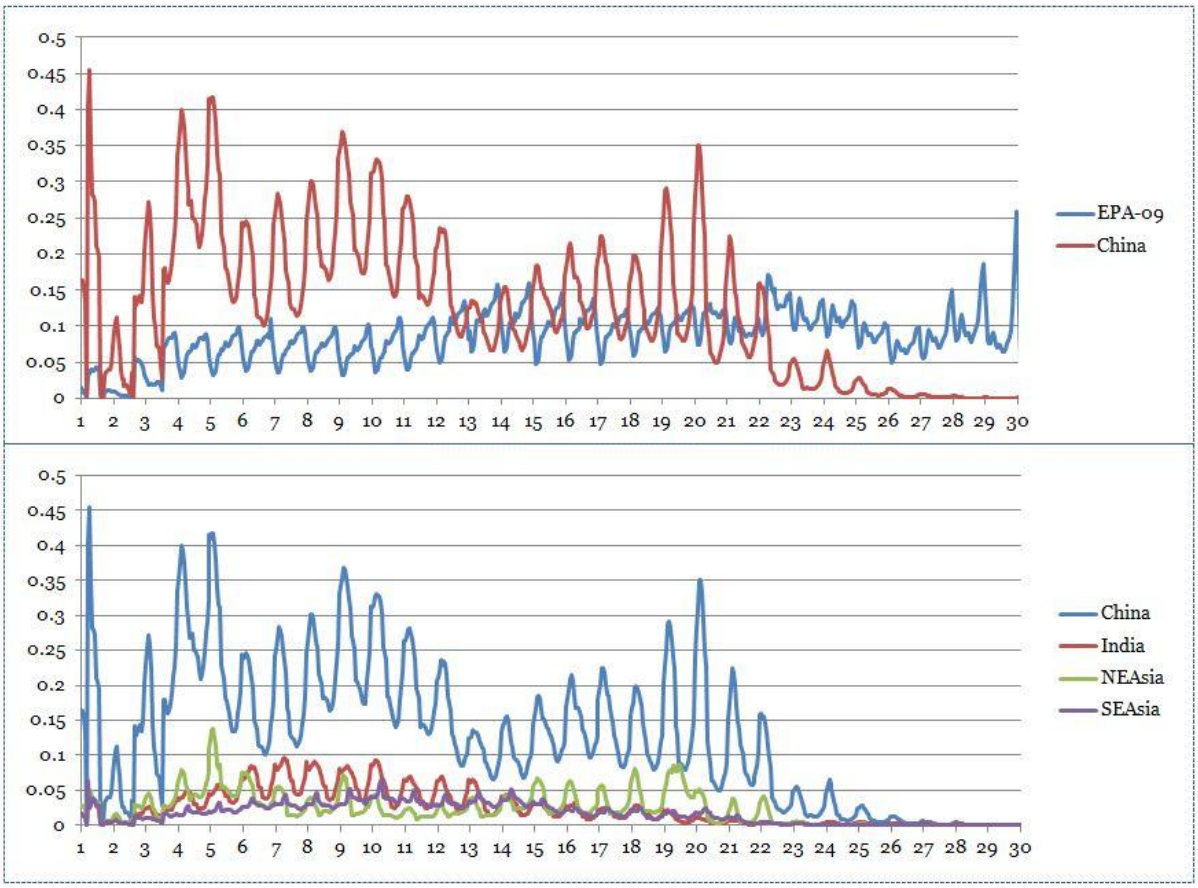

Figure 9. Five Regions of the NOx Emission and Daily Contribution Ratios during 2006/05 to USA O_3

Observations **Surface O3**

Target area **EPA-9, CASTNet sites within EPA-9**

Analysis regions **EPA-9, Arizona, California, and Nevada**

Findings:

1. The two observation scenarios, all samples within the EPA-9 region and CASTNet sites within the EPA-9 region, show similar sensitivities to the NOx emissions.
2. At the state level, the sensitivities show some differences between the two scenarios: The observations at the CASTNet sites show lower sensitivity to the NOx emissions in California and Nevada but higher sensitivity to the NOx emission in Arizona. The variation indicates the representation uncertainty of the CASTNet site observations.

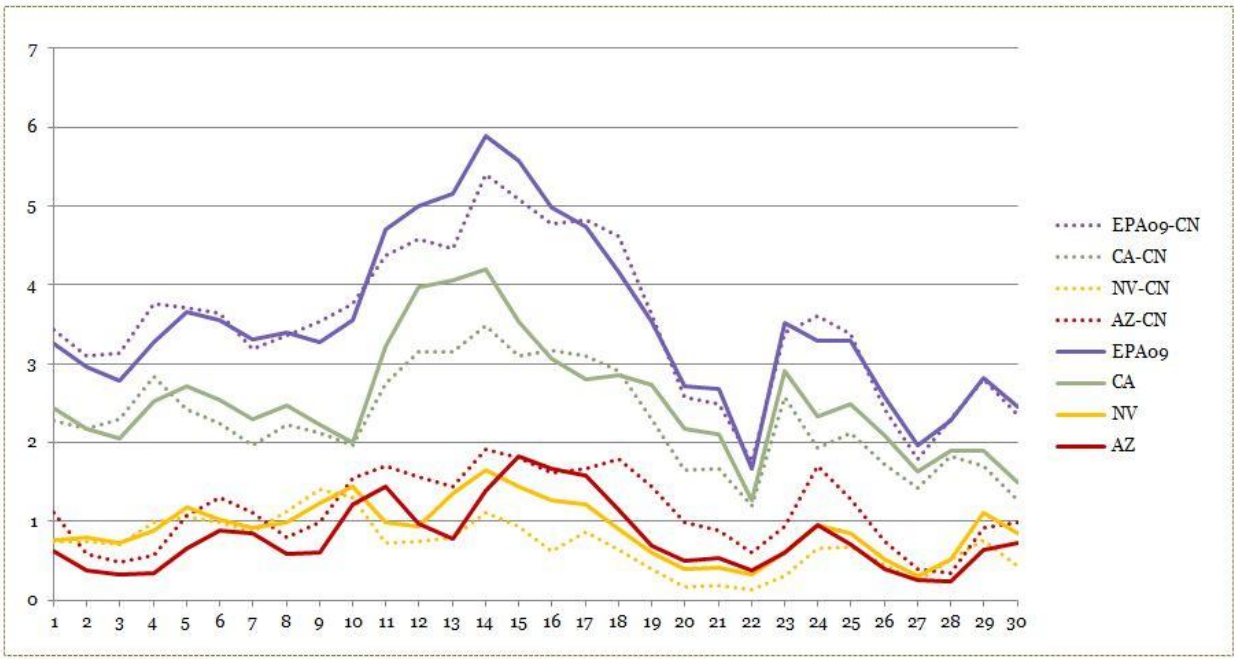

Figure 10. Sensitivity Comparison between Observations at the EPA-9 Region and at CASTNet Sites

(X-axis represents date (2006/05) and Y-axis represents O_3 in ppb)

Observations	**Column O_3 (hourly, during May 2006)**
Target area	**EPA-9**
Analysis duration	**2006/05/01-30**
Analysis regions	**Globe, China, EPA-9**

Findings:

1. The average column ozone over the EPA-9 region is between 45 ppb and 60 ppb.
2. ~5 ppb is sensitive to the global NOx emission.
3. ~1 ppb is sensitive to the EPA-9 NOx emission.
4. ~1 ppb is sensitive to the Chinese NOx emission.

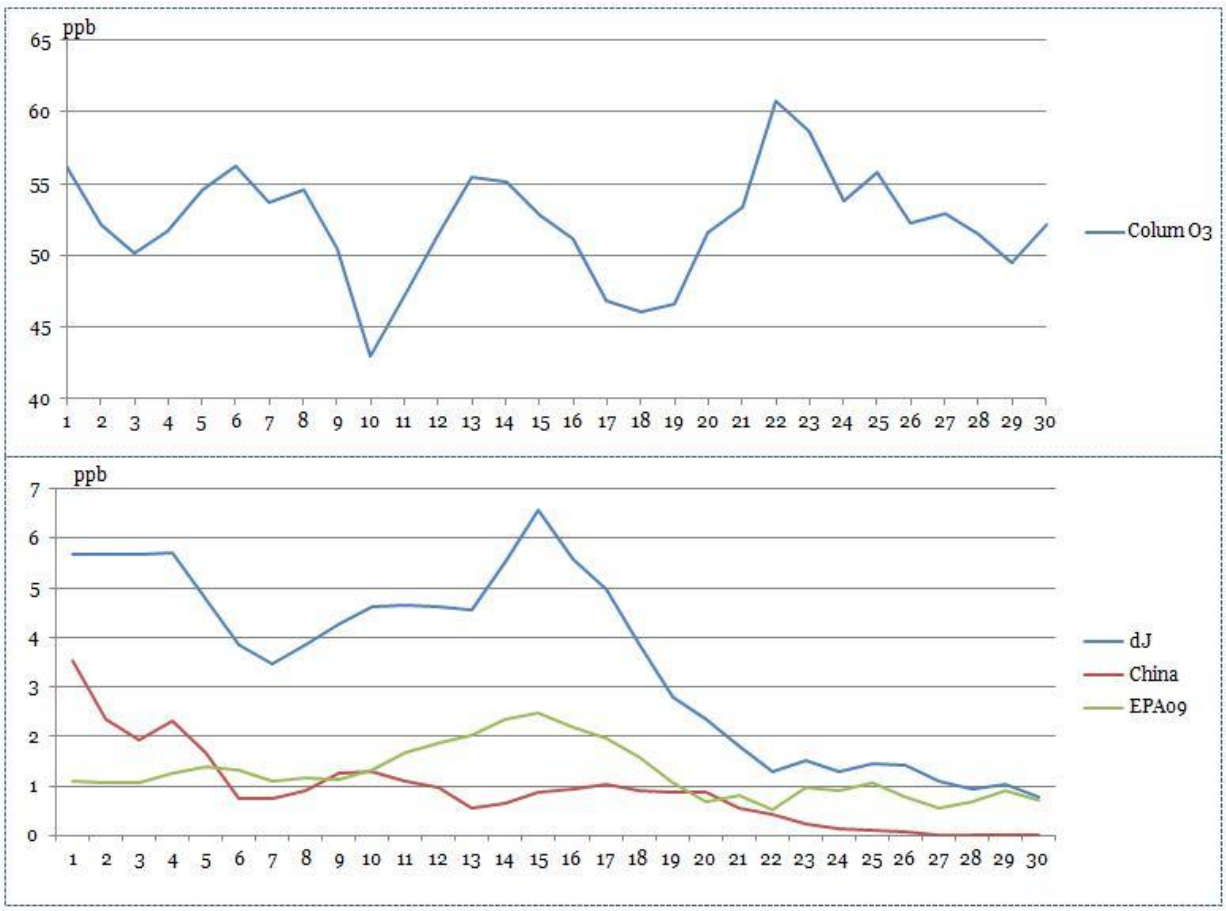

Figure 11. Column O_3 over the EPA-09 Region (Top) and Contributions from NOx Emissions (Bottom)

(The X-axis represents the day of the month (2006/05), and the Y-axis represents the O_3 in ppb.)

Observations	**Column O_3 (hourly, during May 2006)**
Target area	**EPA-9**
Analysis duration	**2006/05/01-30**
Analysis regions	**China, EPA-09, Arizona, California, Nevada**

Findings:

1. It takes ~7 days for the Chinese NOx emission to impact the column ozone in the EPA-9 region.
2. After 20 days, the impact of the Chinese NOx emission is higher than that of EPA-9 region.
3. The majority of the EPA-9 NO_X emission impact is due to the California NO_X emission.

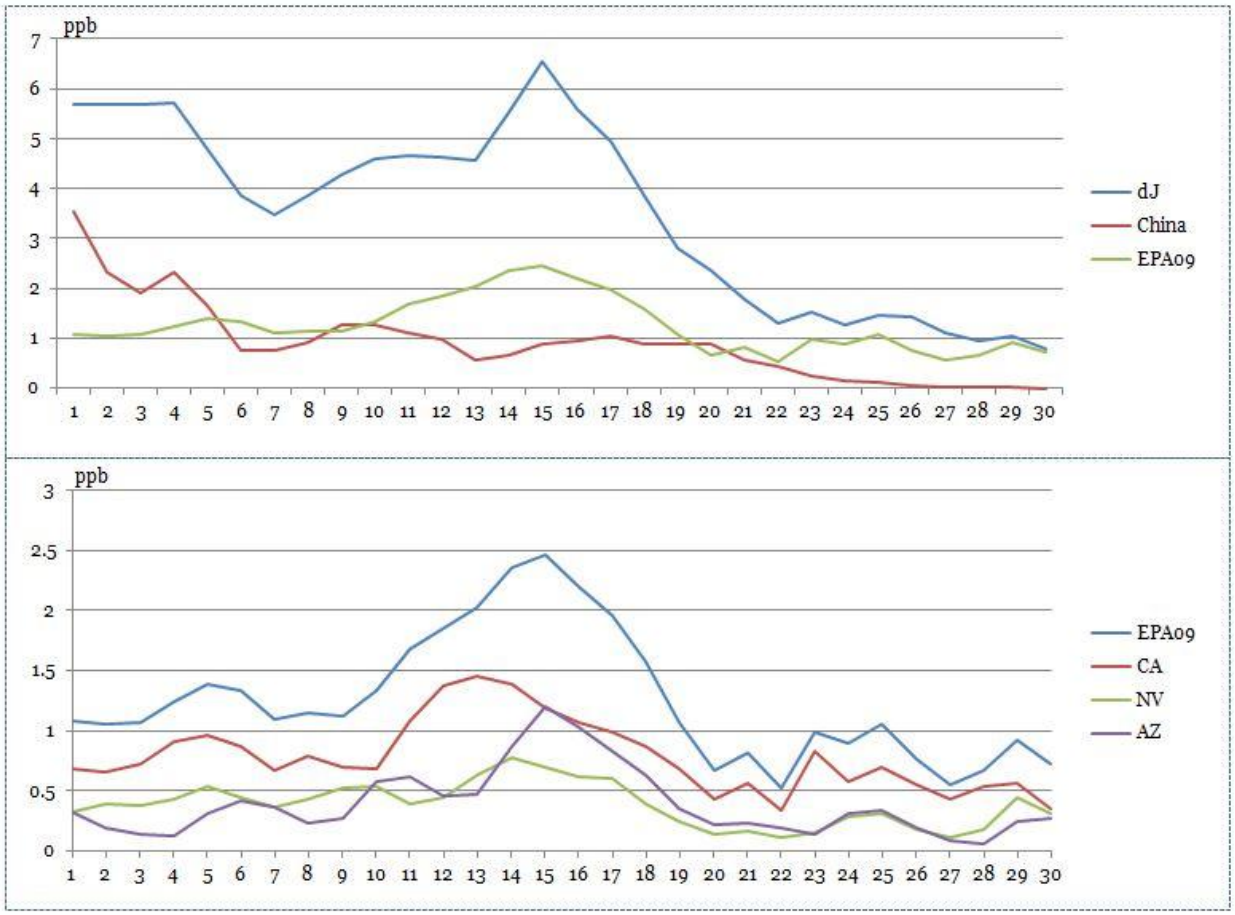

Figure 12. Column O_3 over the EPA-09 Region (Top) and Contributions from NOx Emissions (Bottom)

(The X-axis represents the day of the month (2006/05) and the Y-axis represents the O_3 in ppb.)

Observations	**Column O_3 (hourly, during May 2006)**
Target area	**EPA-9**
Analysis duration	**2006/05/01-30**
Analysis regions	**China, EPA-09**

Findings:

1. There is a strong diurnal signature where the peak influence from the EPA09 NOx occurs at 9AM PST and the peak influence from the Chinese NOx occurs at 10 PM PST.
2. The diurnal signature reflects the diurnal cycle pattern of the NOx emission in Figure 5.

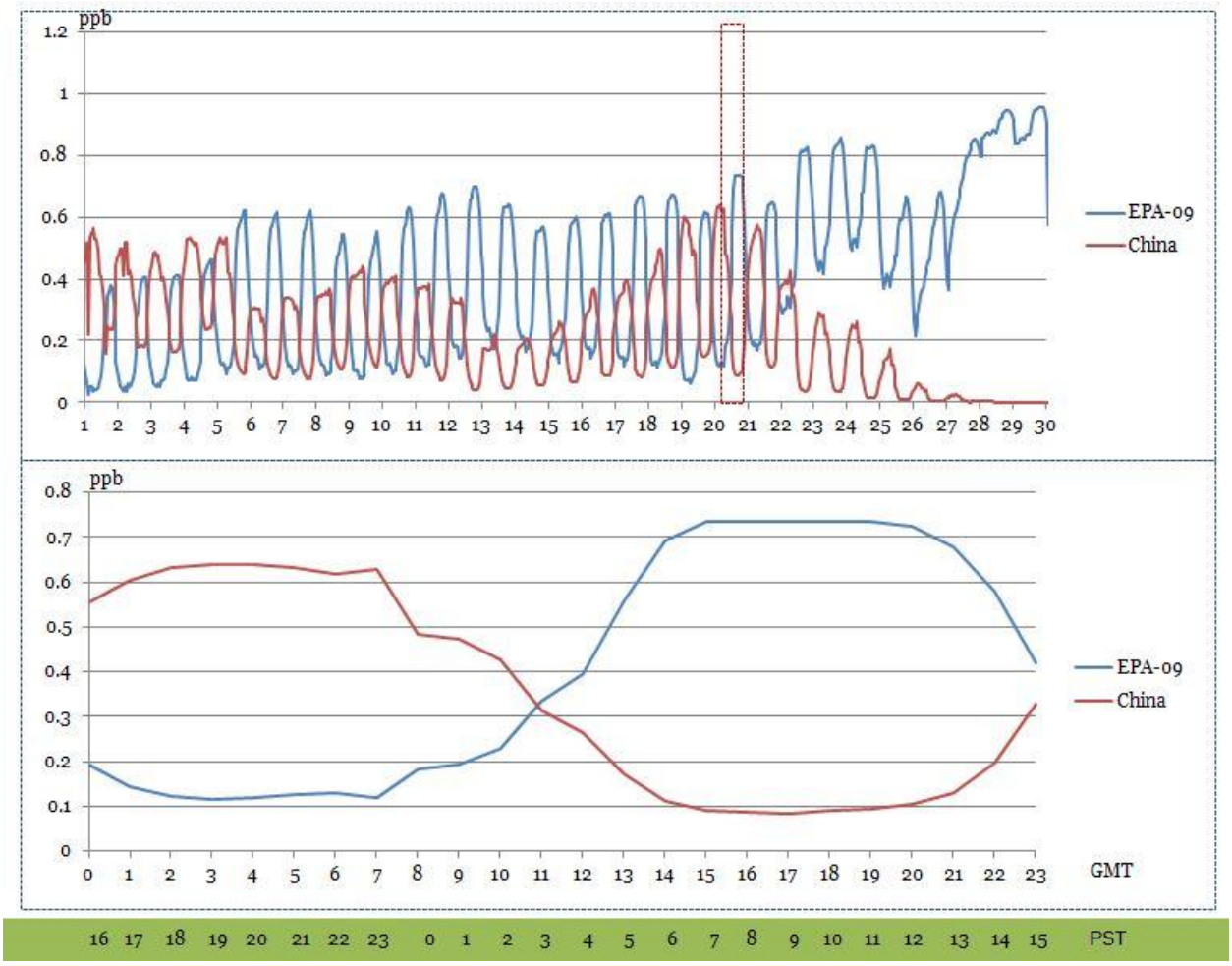

Figure 13. The Column O_3 change in EPA-09 region due to NOx emissions from EPA09 and China for 2006/05 (Top) and 2006/05/20 (Bottom)

Observations	**Surface O_3 and Column O3 (hourly, during May 2006)**
Target area	**EPA-9**
Analysis duration	**2006/05/01-30**
Analysis regions	**Global, China, EPA-09**

Findings:

1. The impact of global NOx and EPA09 NOx to EPA09 O3 at surface shows ~2 ppb higher than over the column.
2. The impact the Chinese NOx to EPA09 03 at surface is negligible, but it is > 1 ppb over the column and the impact starts to appear about one week after the start of the adjoint loop.

Figure 14. Sensitivity Comparison between the Surface O_3 (Top) and Column O_3 Observations (Bottom)

(The dJ represents the daily average O_3 change due to the NOx emissions.)

Observation	**Surface O_3 and Column O_3 (hourly, during May 2006)**
Target area	**EPA-9**
Analysis duration	**2006/05/01-30**
Analysis regions	**Arizona, California, & Nevada**

Findings:

1. The California NOx emission impacts > 50% of the surface ozone but < 40% of the column ozone.
2. The Arizona NOx emission shows much greater impact to the column ozone between May/14-19.

Figure 15. Sensitivity to the State-Wide NOx Emission: Surface O_3 (top) and Column O_3 (Bottom)

4.2 Sensitivity Analysis of Instrument Options

An instrument option is represented with a pressure range and an averaging kernel to formulate an observation operator (H). For example, an instrument whose averaging kernel is a function of the log of the O_3 profile in the unit of "v/v", the observation operator can be simulated by convolving the averaging kernel to the log of the model forecast that has been mapped to the pressure levels of the averaging kernel. The gradient cost is modified by the gradient of the observation operator function that has been mapped back to the model pressure profile.

The sensitivity of the averaging kernel of an observing system was analyzed for three types of instruments, thermal infra-red (TIR), ultra-violet (UV), and visible (VIS) spectrometers. Figure 16 shows the diagonal vector of the averaging kernel of the three instrument types where the X-axis represents 120 pressure-level bins (1000 hPa to 0.0 hPa), and the Y-axis represents the normalized amplitude. Figure 17 compares the sensitivity of the observed ozone from the above three instruments to the ideal instrument where the observed ozone of each instrument is simulated by convolving the ideal observation with the respective averaging kernel.

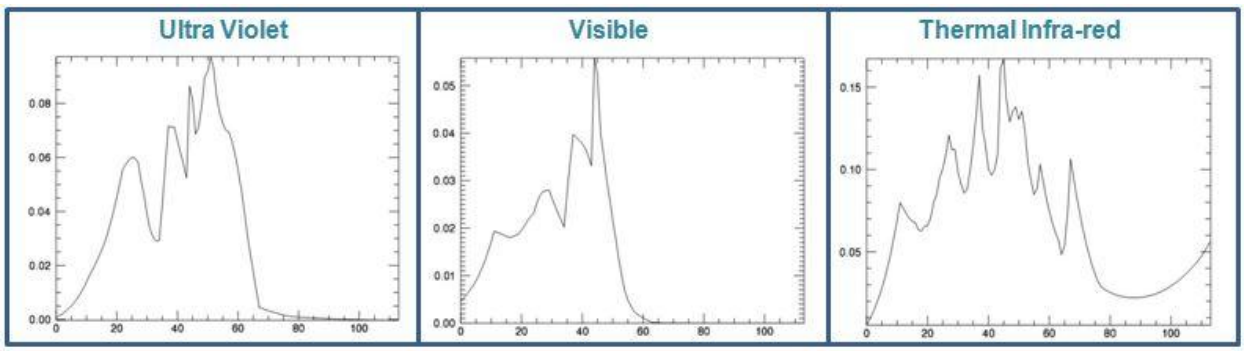

Figure 16. Diagonal Vector of the Averaging Kernel of Three Instruments
(X-axis represents the pressure levels and the Y-axis represents the amplitude)

Observations	**Column O_3 at 3:00 PM on 2007/07/26**
Target area	**Washington D.C.**
Analysis duration	**2007/07/21- 26**
Analysis instruments	**IDEAL, TIR, UV, VIS**

Findings:

1. The ideal case indicates that the column O_3 in Washington, D.C. is affected by the NOx emissions in N. America throughout the 6 day period, and the strongest emission sources were three days away.
2. The TIR is >90% responsive to the distant emission sources and <70% responsive to the near ones.
3. The UV is as responsive as TIR over the near emission sources.
4. The VIS responds poorly to all emission sources.

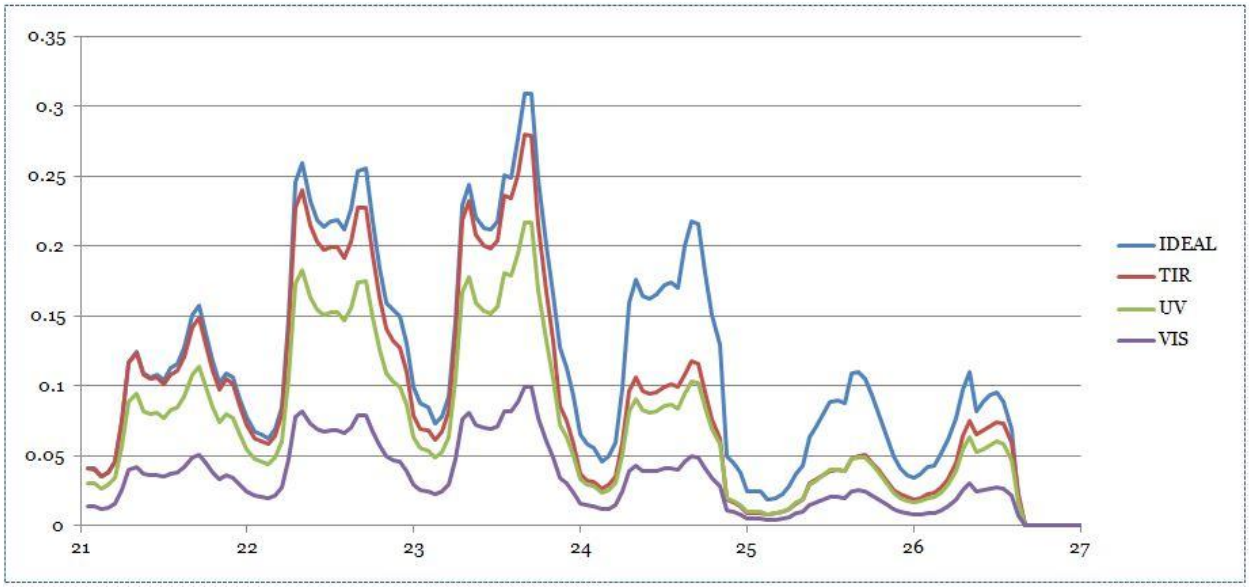

Figure 17. Sensitivity Comparison of the Three Instruments Relative to an Ideal Instrument
(X-axis represents the day in 2006/07 and Y-axis represents the fractional sensitivity)

5 Appendices

Appendix A. Checkpoint files

File name	input	output	used by				New File	
adjoint								
bg	STT	TRACER(IIPAR,JJPAR,LLPAR)	subdriver_fwd_4d	REAL*8	BPCH2_CHK		WRITE_STT_CHKFILE	
chem	STT	TRACER(IIPAR,JJPAR,LLPAR)	subdriver_fwd_4d	REAL*8	BPCH2_CHK		WRITE_STT_CHKFILE	
chemp1								
chemp2								
chemp3								
chemp								
conv	STT	TRACER(IIPAR,JJPAR,LLPAR)	subdriver_fwd_4d	REAL*8	BPCH2_CHK		WRITE_STT_CHKFILE	
csp1	CSPEC	TRACER(ITLOOP,IGAS)	gasconc	REAL*8	BPCH2_CSP		WRITE_CSP_CHKFILE	
csp2	CSPEC	TRACER(ITLOOP,IGAS)	chemdr	REAL*8	BPCH2_CSP		WRITE_CSP_CHKFILE	
curr	STT	TRACER(IIPAR,JJPAR,LLPAR)	subdriver_fwd_4d	REAL*8	BPCH2_CHK		WRITE_STT_CHKFILE	
diffpert								
emisdep								
emisrate	EMIS_RATE	TRACER(ITLOOP,IND)	chemdr	REAL*8	BPCH2_CSP	IND = 40	MAKE_EMISRATE_CHKFILE	x
f								
fpbl	FP	TRACER(IIPAR,JJPAR)	pbl_mix_mod	REAL*8	BPCH2_CSP		MAKE_FPBL_CHKFILE	x
hsave	HSAVE_KPP	TRACER(IIPAR,JJPAR,LLPAR)	chemdr	REAL*4	BPCH2	JJLOOP=1,NTT	MAKE_HSAVE_CHKFILE	x
imix	IM	TRACER(IIPAR,JJPAR)	pbl_mix_mod	REAL*8	BPCH2_INT		MAKE_IMIX_CHKFILE	x
indemis								
obs								
optz	STT*TCVV/AD	TRACER(IIPAR,JJPAR,LLPAR)	subdriver_fwd_4d	REAL*4	BPCH2		MAKE_OPT_CHKFILE	
optz2								
orig	STT*TCVV/AD	TRACER(IIPAR,JJPAR,LLPAR)	subdriver_fwd_4d	REAL*4	BPCH2		MAKE_OPT_CHKFILE	
part								
pert								
pres	TMP_PRESS	TRACER(IIPAR,JJPAR)	transport	REAL*4	BPCH_2D		MAKE_PRESSURE_CHKFILE	x
rrate	R_KPP	TRACER(NTT,NREACT)	chemdr	REAL*8	BPCH2_CSP		MAKE_RRATE_CHKFILE	x
srcemis								
totemis								
upbdflx	STT_TMP	TRACER(IIPAR,JJPAR,LLPAR)	linoz_mod.f	REAL*8	BPCH_CHK	N=1,2	MAKE_UPBDFLX_CHKFILE	x

Appendix B. NOx Emission Inventory

The GCA integrates a wide range of emission models selecting specific sectors and applying sector-specific temporal scaling. For example, the GCA integrates twelve sectors of Edgar v4.2 and four sectors of Streets applying sector-specific temporal scaling. The GCA also integrates region-specific emission models. For example, the Streets emission model is used only for the South East Asia region.

Edgar v4.2

Type	Sector	Temporal scaling	Misc. description
Fuel combustion (9 types)	Industry	hourly	
	Power generation	hourly	
	conversion	annual	
	residential	hourly	
	road transport	hourly	
	non-road transport	hourly	
	aircraft		Not used
	shipping		Not used
	Oil production	annual	
Other sources (5 types)	Iron and steel production	annual	
	Chemical production	annual	
	Cement production	annual	
	Pulp & paper production	annual	
	Waste incineration	annul	

Streets (David Streets)

Type	Sector	Temporal scaling	Misc. description
Anthro	industry	annual + monthly	SE Asia
	power	annual + monthly	SE Asia
	residence	annual + monthly	SE Asia
	transport	annual + monthly	SE Asia

Appendix C. Tracer name list

Tracer ID	*Name*	*g/mole*	*Description*
1	Nox	46	$NO+NO_2+NO_3+HNO_2$
2	Ox	48	$O_3+NO_2+2NO_3$
3	PAN	121	Peroxyacetyl Nitrade ($C_2H_3NO_5$)
4	CO	28	Carbon Monoxide
5	ALK4	12	Active Receptor-Like Kinase 4
6	ISOP	12	Isoprene (C_5H_8)
7	HNO_3	63	Nitric Acid
8	H_2O_2	34	Hydrogen Peroxide
9	ACET	12	Acetone (C_3H_6O)
10	MEK	12	Methyl Ethyl Ketone (C_4H_8O)
11	ALD2	12	Acetaldehyde (C_2H_4O)
12	RCHO	58	Lumped Aldehyde
13	MVK	70	Methyl Vinyl Ketone
14	MACR	70	Methacrolein (C_4H_6O)
15	PMN	147	Peroxy methacryloyl Nitrade
16	PPN	135	Lumped Peroxypropionyl Nitrade
17	R4N2	119	Lumped Alkyl Nitrade
18	PRPE	12	Lumped >=C_3 Alkenes
19	C_3H_8	12	Propane
20	CH_2O	30	Formaldehyde
21	C_2H_6	12	Ehtane
22	N_2O_5	105	Dinitrogen Pentoxide
23	HNO4	79	Pernitric Acid
24	MP	48	Methyl Hydro Peroxide (CH_4O_2)
25	DMS	62	HNO3
26	SO_2	64	Sulfur Dioxide
27	SO_4	96	Sulfate
28	SO_{4s}	96	Sulfate on surface of sea-salt aerosol
29	MSA	96	Methyl Sulfonic Acid
30	NH_3	17	Ammonia
31	NH_4	18	Ammonium
32	NIT	62	Inorganic Sulfur Nitrates
33	NITs	62	Inorganic Nitrates on surface of sea-salt aerosol
34	BCPI	12	Hydrophilic black carbon aerosol
35	OCPI	12	Hydrophilic organic carbon aerosol
36	BCPO	12	Hydrophobic black carbon aerosol
37	OCPO	12	Hydrophobic organic carbon aerosol
38	DST1	29	Dust aerosol, Reff=0.7 microns

Tracer ID	*Name*	*g/mole*	*Description*
39	DST2	29	Dust aerosol, Reff=1.4 microns
40	DST3	29	Dust aerosol, Reff=2.4 microns
41	DST4	29	Dust aerosol, Reff=4.5 microns
42	SALA	36	Accumulation mode sea salt aerosol (Reff=0.1-2.5 microns)
43	SALC	36	Coarse mode sea salt aerosol (Reff=2.5-4 microns)

Appendix D. Acronyms and Abbreviations

AEF	Annual Emission Factor
CAC	Common Air Contaminants
CASTNet	Clean Air Status and Trends Network
CONUS	continental United States
CTH	cloud top height
EDGAR	Emissions Database for Global Atmospheric Research
EMEP	European Monitoring and Evaluation Program
GCA	GEOS-Chem-Adjoint version 34 system
GC/OC	Gas Chromatography /Organic Carbon
GEO-CAPE	Geostationary Coastal and Air Pollution Events
GEOS-5	Goddard Earth Observing System version 5
GFED	Global Fire Emission Database
ICOADS	International Comprehensive Ocean-Atmosphere Data Set
ISOP	Isoprene (chemical compound: C_5H_8)
MEGAN	Model of Emissions of Gases and Aerosols from Nature
MONOT	Monoterpene (chemical compound: $C_{10}H_{16}$)
NEI	National Emissions Inventory
OSSE	Observing System Simulation Experiment
TIR	thermal infrared
UV	ultraviolet
VIS	visible
V/V	volume/volume